Planetary Systems in the Universe - Observation, Formation and Evolution
Proceedings IAU Symposium No. 202, ©2004 IAU
Alan Penny, Pawel Artymowicz, Anne-Marie Lagrange, & Sara Russell, eds.

Companion Detection Limits with Adaptive Optics Coronagraphy

B. R. Oppenheimer

Astronomy Dept., University of California-Berkeley, Berkeley, CA 94720, USA

R. G. Dekany, M. Troy

Jet Propulsion Laboratory, Oak Grove Dr., Pasadena, CA 91125, USA

T. Hayward, B. Brandl

Astronomy Dept., Cornell University, Ithaca, NY 11410, USA

Abstract. We present a study of the Palomar Adaptive Optics System and the PHARO near infrared camera in coronagraphic mode. The camera provides two different focal plane occulting masks–opaque circular disks 0.43 and 0.97″ across. Three different pupil plane apodizing masks (Lyot masks) are also provided. The six different combinations of Lyot mask and focal plane mask suppress differently the point spread function of a bright star centered on the focal plane mask. We obtained images of the bright nearby star Gliese 614 with all six different configurations in the K filter. We measured the dynamic range achievable with these configurations. Within 2.5″, the dynamic range is at least 8 magnitudes at the 5σ level and as high as 12 in a 1 s exposure. This represents a substantial gain over similar techniques without adaptive optics.

1. Introduction

The basic idea behind a coronagraph is that a focal plane stop is introduced with approximately the size of the stellar image. This blocks out most of the light of the star. However, light is scattered in the atmosphere and in the telescope optics, so a Lyot mask is introduced as well, to reduce the broad halo of light from the star.

With the advent of adaptive optics, it is now possible to achieve high dynamic ranges at extremely small separations from a given star, because we can now design coronagraphs that are optimized for the diffraction limit. The adaptive optics system provides a nearly diffraction limited image (fractions of an arcsecond in width) on top of a seeing-disk halo. A coronagraph, fitted behind an adaptive optics system, therefore, can permit one to probe the vicinities of nearby stars on the spatial scale of the solar system. With this in mind, the Palomar High Angular Resolution Observer (PHARO) infrared camera, which is the principal instrument for the Palomar Adaptive Optics System (PALAO, Dekany et al. 1998), was designed with a coronagraphic imaging mode.

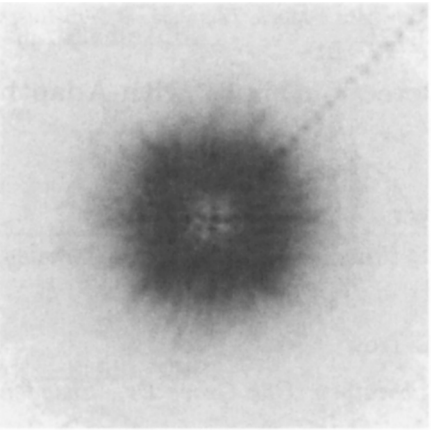

Figure 1. A 256×256 pixel portion of the reduced K-band image of Gliese 614 with the 0.97" focal plane mask and the big Lyot stop. The pixel scale is 25 mas and total exposure time is 180s. Artificial point sources have been introduced as Airy functions along the radius 45° right of up. These artificial sources are introduced at the 5σ detection level and are used to produce the dynamic range functions in Fig. 2.

The coronagraph on PHARO permits six different configurations: there are two different focal plane stops, 0.43" and 0.97" in diameter, and three different Lyot masks, which downsize the pupil by 100% (the standard imaging mask), ~90% (the "medium" Lyot mask) and ~80% (the "big" mask) of the outer radius. The pupil masks in PHARO not only mask out the outer part of the pupil but also expand the inner part, which covers the secondary obscuration. For example, the big mask reduces both the outer diameter of the annular pupil by 1/5 and increases the inner diameter by 1/5 of its value in the standard mask.

We have conducted observations of the star Gliese 614 (HD 145675, BD+44 2549, a $V = 6.67$, K0V star at 18.14 pc with no known companions or surrounding diffuse emission) in the K band using PHARO and PALAO in order to assess experimentally the dynamic range possible with this instrument.

2. Assessment of the Dynamic Range

In order to assess the dynamic range of the images, we used a technique previously outlined (Oppenheimer 1999). We introduced artificial point sources, with photon noise and read noise matching the detector characteristics, at various radial distances from the central, obscured star (Fig. 1). The goal of these measurements is to produce the 5σ detection limits as a function of radius from the star. The detection limits are specified as the magnitude difference between the star and the putative companion. Near the star, the star light is the limiting factor, providing a bright background and increasing the noise in that region. Beyond about 2", the star is relatively unimportant and the instrument detection limits determine the maximum possible dynamic range.

Fig. 2 shows the azimuthally averaged dynamic range functions for the six possible settings and an integration time of 1 second. One second is chosen

https://doi.org/10.1017/S0074180900217592 Published online by Cambridge University Press

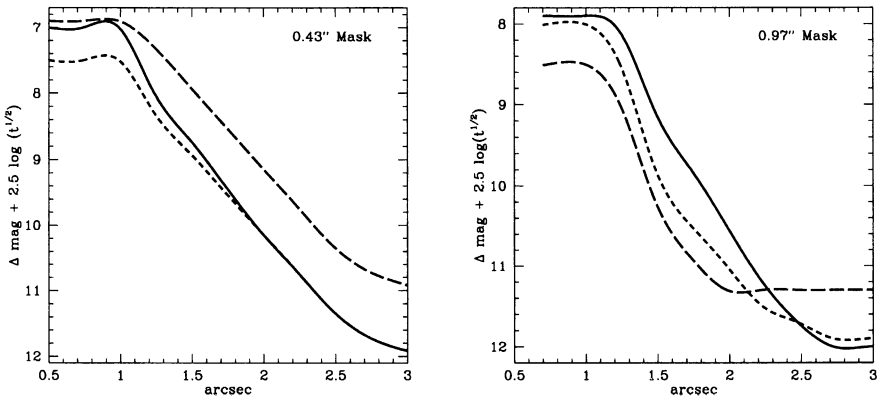

Figure 2. 5σ detection limits for faint point sources near bright stars in K band, (a, left) with the 0.43" focal plane mask and (b, right) with the 0.97" mask. The three curves correspond to the standard Lyot stop (solid line), the medium Lyot stop (short dashed line) and the big Lyot stop (long dashed line). The curve is presented in terms of magnitude difference from the star for an integration time of 1 second. The ordinate indicates the dynamic range as a function of integration time, t, in seconds. The variation in the curves as a function of azimuthal angle is less than .2 mag in all cases.

to allow for ease in modifying the curves by integration time. To adjust the curve for a given exposure time, t, simply shift the y-axis (Δ mag) by adding $2.5log(t^{1/2})$, where t is in seconds. In the large radius limit, where the dynamic range curve levels off, the detector limit is reached. This part of the curve will simply follow the immediately preceding part (at lower radius) in a linear fashion for deeper exposure times.

There are several important features of Fig. 2 to note. The larger mask and larger Lyot stop provide superior results by up to a magnitude. In addition, it should be noted that both figures demonstrate the strong effect of the Lyot stop. In Fig. 2a the occulting mask and the Lyot stop are not well matched to the instrument. As a result, the big Lyot stop simply causes the telescope to behave as if it had a smaller pupil, with poorer detection limits at all radii. The medium stop increases the dynamic range at small radii, but eventually matches the effect of the standard Lyot stop. In Fig. 2b, the big Lyot stop clearly limits the ultimate detection limit of the image in the large radius regime, because it downsizes the telescope aperture. However, at low radii, it provides superior suppression of the central star's point spread function. Thus, the curve corresponding to the big Lyot stop in Fig. 2b starts out lower (higher dynamic range) than the others, but ultimately crosses the medium and standard Lyot stop curves. This clearly demonstrates that one must carefully choose the proper setting depending upon what radius is of interest to the observing program, and that the optical matching of the Lyot stop and focal plane mask is absolutely critical.

The big Lyot stop also provides a much faster fall-off of the central star point spread function. In Fig. 2b the slope of the curves is much steeper than

https://doi.org/10.1017/S0074180900217592 Published online by Cambridge University Press

in Fig. 2a. We note again that, in K band, the 0.97" mask is about 9 times the diffraction limit and the 0.43" mask is 4 times the diffraction limit. It follows that in J band, where the 0.43" mask is $9\lambda/D$, that the medium Lyot stop and the 0.43" mask will provide results comparable to the 0.97" mask and the big Lyot stop in the K band at similar Strehl ratios.

One interesting feature in the dynamic range curves is the leveling off below the one arcsecond radius. This is due to the apparent "plateau" in the point spread function inside the waffle pattern. While in most cases this plateau is not important, it is the dominant factor in these high dynamic range situations. Furthermore, the bump at nearly one arcsec, most clearly seen in the curve corresponding to the 0.43" mask and the standard Lyot stop, is a direct manifestation of the waffle pattern.

The conclusions and results just described are easily understood if one considers the coronagraph from the point of view of Fourier optics. After the focal plane mask, the pupil is reimaged (a Fourier transform of the focal plane). The unocculted light from the central star is now largely concentrated at the edge of the pupil, the high frequency part of the pupil plane (low spatial frequency in the focal plane). The Lyot stop acts as a low-pass filter in the pupil plane by blocking out this light. As a result, the low spatial-frequency component in the focal plane is subdued. In other words, the Lyot stop acts to suppress the broad wings of the on-axis point spread function. The effect is clearly seen in Fig. 2b where the big Lyot stop provides a clear improvement over the standard one. (n. b. the standard Lyot stop in these plots is essentially equivalent to direct imaging without the coronagraph, since the coronagraph is only acting to suppress the peak of the stellar image.)

We must note that the central star used in these cases was a K0V star with $V = 6.67$. If a fainter star is used, the same curves will apply, but the limiting magnitude (level part of the curve) will be lowered to limit the dynamic range at smaller radii. For example, if the limiting magnitude of the image is smaller than the central star magnitude plus 8, the image's limiting magnitude will be the dominant effect at all radii.

References

Dekany, R. G., Brack, G., Palmer, D., Oppenheimer, B. R., Hayward, T. L., & Brandl, B. 1998, Proc. SPIE, 3353, 56

Oppenheimer, B. R. 1999, Ph. D. Thesis, California Institute of Technology